JACS
JOURNAL OF THE AMERICAN CHEMICAL SOCIETY

COMMUNICATION

pubs.acs.org/JACS

NMR Cross-Correlated Relaxation Rates Reveal Ion Coordination Sites in DNA

Radovan Fiala,*[,†] Naďa Špačková,[‡] Silvie Foldynová-Trantírková,[§] Jiří Šponer,[†,‡] Vladimír Sklenář,[†] and Lukáš Trantírek*[,∥]

[†]National Centre for Biomolecular Research and CEITEC, Masaryk University, Brno, Czech Republic

[‡]Institute of Biophysics, Academy of Sciences of the Czech Republic, Brno, Czech Republic

[§]Biology Centre, Academy of Sciences of the Czech Republic, České Budějovice, Czech Republic

[∥]Department of Chemistry, Utrecht University, Utrecht, The Netherlands

Supporting Information

ABSTRACT: In this work, a novel NMR method for the identification of preferential coordination sites between physiologically relevant counterions and nucleic acid bases is demonstrated. In this approach, the NMR cross-correlated relaxation rates between the aromatic carbon chemical shift anisotropy and the proton−carbon dipolar interaction are monitored as a function of increasing Na^+, K^+, and Mg^{2+} concentrations. Increasing the counterion concentration modulates the residence times of the counterions at specific sites around the nucleic acid bases. It is demonstrated that the modulation of the counterion concentration leads to sizable variations of the cross-correlated relaxation rates, which can be used to probe the site-specific counterion coordination. In parallel, the very same measurements report on the rotational tumbling of DNA, which, as shown here, depends on the nature of the ion and its concentration. This methodology is highly sensitive and easily implemented. The method can be used to cross-validate and/or complement direct but artifact-prone experimental techniques such as X-ray diffraction, NMR analysis with substitutionary ions, and molecular dynamics simulations. The feasibility of this technique is demonstrated on the extraordinarily stable DNA mini-hairpin d(GCGAAGC).

Interactions of polyanionic DNA with counterions influence DNA stability and structure by modulating the thermodynamics of the noncovalent interactions.[1,2] The interactions between counterions and DNA also play an important role in biological processes such as DNA recognition by proteins or small molecular ligands.[3] Although this is a subject of great interest, an understanding of the rules that govern interactions between nucleic acids (NAs) and ions remains elusive.[2] The major impediment to the characterization of these interactions, which are transient and weak in nature, is a general lack of unbiased techniques allowing their investigation.

High-resolution information on DNA−ion interactions usually comes from either X-ray crystallography or solution NMR and EPR analysis.[4−8] Unfortunately, the results of these methods are often biased. The low water content of crystalline samples used in X-ray studies along with the use of unnaturally occurring salts and precipitants facilitating crystallization frequently leads to changes in DNA structure, biasing the readout on physiologically relevant DNA solvation.[9] A low degree of hydration has also been shown to change the nature of the DNA−ion interactions, favoring direct interactions between DNA and ions over the water-mediated ion−DNA interactions observed in solution.[10]

In contrast to X-ray studies, NMR and EPR measurements can be performed under physiological conditions. Unfortunately, the NMR and EPR properties of the physiologically relevant counterions (e.g., Na^+, K^+, Mg^{2+}) do not allow the application of standard techniques for identification of their interaction sites. These limitations are usually overcome by the application of mimicking systems (e.g., NH_4^+ for monovalent ions or Mn^{2+} for Mg^{2+}).[5,7,8]

This report describes a novel, simple approach based on monitoring of the NMR cross-correlated relaxation rates (Γ) between the aromatic carbon chemical shift anisotropy (CSA) and the proton−carbon dipolar interaction as a function of increasing ion concentration that can be used to identify the binding sites between physiologically relevant counterions and DNA. In parallel, the very same measurements report on the counterion-dependent hydrodynamics of DNA. The method is demonstrated on the extraordinarily stable DNA mini-hairpin d(GCGAAGC)[11,12] [Figure S1 in the Supporting Information (SI)].

If it is assumed that the molecule undergoes isotropic overall motion and that the internal motions are much faster than the overall tumbling of the molecule, Γ can be expressed as[13]

$$\Gamma_{C,CH}^{CSA,DD} = -\frac{4}{15}\left(\frac{\mu_0\hbar}{4\pi}\right)\frac{\gamma_H\gamma_C{}^2}{r_{C-H}{}^3} B_0\sigma_{C,CH}S^2\tau_c \qquad (1)$$

where γ_H and γ_C denote the magnetogyric ratios of the ^1H and ^{13}C nuclei, respectively, r_{C-H} is the C−H internuclear distance, B_0 is the strength of the magnetic field, S^2 is the generalized order parameter describing motion of the C−H vector on the picosecond−nanosecond time scale, τ_c is rotational correlation time, and $\sigma_{C,CH}$ is the effective CSA (see eq S3 in the SI).

Considering that the fluctuations of C−H vectors (described by S^2) take place on a time scale that is the same as or shorter than the expected residence times of binding ions and that $\sigma_{C,CH}$ is one of the NMR parameters that is most sensitive to changes in

Received: March 16, 2011
Published: August 08, 2011

dx.doi.org/10.1021/ja202397p | J. Am. Chem. Soc. 2011, 133, 13790–13793

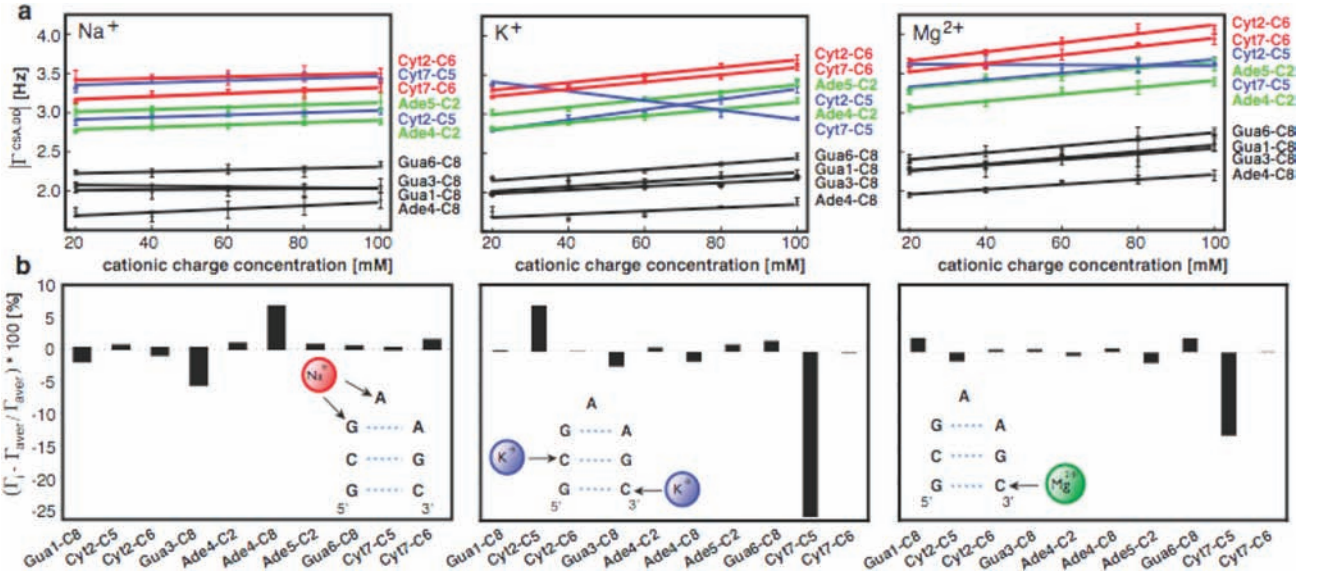

Figure 1. (a) $|\Gamma|$ as a function of Na^+, K^+, and Mg^{2+} concentrations. The salt concentration is expressed as the cation concentration multiplied by its charge. (b) Site-specific differences between Γ_i and the value averaged over all probed sites (Γ_{aver}) as a function of increasing salt concentration from 20 to 100 mM NaCl and KCl and 10 to 50 mM $MgCl_2$. The differences are given in % and report on the relative site-specific variability of $(\Gamma_i - \Gamma_{aver})$ with respect to Γ_{aver}. The values of Γ were corrected for an increase in macroscopic viscosity due to increasing salt concentration.

the electron distribution in the vicinity of the probed site, we presumed that the product $\sigma_{C,CH} \cdot S^2$, which is responsible for the site specific-modulation of Γ, would be a very sensitive reporter for the presence of ions in the vicinity of the DNA bases.

To test this idea, Γ was measured for the C6 and C5 sites of cytosines, C8 in purines, and C2 in adenosines in the presence of 20−100 mM NaCl and KCl and 10−50 mM $MgCl_2$. For all ion types and most of the measured carbon atoms, the Γ values increased linearly with ion concentration over the given concentration ranges (Figure 1a). However, there were two exceptions, namely, Γ for the C8 carbon of Gua3 in the presence of Na^+ and Γ for the C5 carbon of the terminal Cyt7 in the presence of K^+ and Mg^{2+} (Figure 1a). To quantify the relative differences among the Na^+, K^+, and Mg^{2+} samples, the experimentally acquired Γ values were corrected for viscosity changes due to the presence of the salt (see the SI). This step is essential because both the type and the concentration of the added salt determine the overall macroscopic viscosity of the NMR sample, which modulates the correlation time of the DNA and thus the measured value of Γ. Subsequent analysis revealed that in the presence of Na^+, the values of Γ did not vary significantly (typically <3%) with increasing Na^+ concentration. In the presence of K^+, the values of Γ generally increased on average by 11.5% from their original values as the salt concentration increased from 20 to 100 mM. In the presence of Mg^{2+}, the observed increase in the Γ values with increasing cationic Mg^{2+} strength from 10 to 50 mM reached, on average, 7.5% of the original values (Figure S2).

To investigate whether the observed differences in the response of Γ resulted from changes in the molecular geometry induced by different ions, the spectral patterns of the 2D $^1H-^{13}C$ heteronuclear single-quantum correlation (HSQC) spectra of the aromatic and C1′ regions, the 1D ^{31}P spectra, and the inter-residual distances extracted from nuclear Overhauser effect spectroscopy (NOESY) spectra of the hairpin were compared in the presence of 100 mM NaCl and KCl and 50 mM $MgCl_2$ (Figures S3−S5 and Tables S2 and S3). The ^{31}P, ^1H, and ^{13}C chemical shifts (δ) and the NOEs within the hairpin were virtually identical in the presence of 100 mM NaCl and 100 mM KCl, indicating that the overall folding topology and the structure of the hairpin are unaffected by the nature of the monovalent ion. While the comparison of spectral patterns revealed substantial differences between the Na^+/K^+ and Mg^{2+} solutions with respect to aliphatic ^{13}C and ^{31}P δ values (Figure S5 and Table S2), the inter-residual NOEs and aromatic ^{13}C δ values were virtually unaffected, with the exception of the terminal Cyt7, which, as indicated by the presence of exchange peaks in the NOESY spectra, was subjected to chemical exchange (Figures S3 and S4 and Table S3). A plausible explanation for these observations is that although Mg^{2+} affects the geometry of the phosphodiester backbone, the changes in the phosphodiester backbone are not transferred to either the glycosidic torsions or the stacking arrangements of the bases in the tightly packed hairpin structure.

The fact that the increases in Γ with increasing ion concentration were very similar for most of the atoms indicates that the increase results from a mechanism common to the entire molecule (i.e., an increase in the overall correlation time τ_c). This interpretation is supported by quantitative analysis of autorelaxation rates (Table S4).

Although the values of Γ appear to be uniformly modulated by the counterion concentrations, quantitative analysis of the Γ values revealed site-specific differences in their response to increasing salt concentration. Figure 1b shows relative site-specific variations in Γ due to increased ion concentrations from 20 to 100 mM (Na^+ and K^+) and 10 to 50 mM (Mg^{2+}). In the presence of Na^+, the Γ values were mostly insensitive to increasing salt concentration. However, there were two exceptions, namely, $\Gamma_{C8,C8-H8}$ from Gua3 and $\Gamma_{C8,C8-H8}$ from Ade4. The values of Γ from Gua3 decreased with increasing ion concentration. In contrast, the value of Γ from Ade4 significantly increased relative to Γ_{aver}. The site-specific effects observed for

dx.doi.org/10.1021/ja202397p |J. Am. Chem. Soc. 2011, 133, 13790–13793

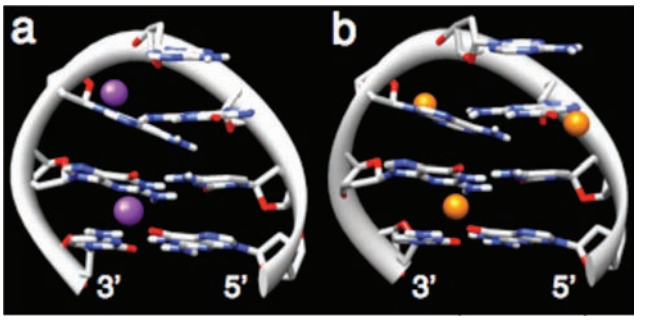

Figure 2. Preferential coordination sites for (a) K^+ and (b) Na^+ ions as revealed by MD simulations performed with excess cations (~0.30 M).

Ade4 and Gua3 in the presence of Na^+ were considerably diminished in both K^+ and Mg^{2+} solutions. On the other hand, $\Gamma_{C5,C5-H5}$ from Cyt2 and Cyt7 and $\Gamma_{C5,C5-H5}$ from Cyt7 were notably affected by increasing K^+ and Mg^{2+} concentrations. In the cases of K^+ and Mg^{2+} ions, the affected sites, representing the GpC steps, directly correspond to the preferential interaction sites of K^+ and Mg^{2+} ions.[14] Our observation of different site-specific preferences for various ions is in agreement with other experimental data.[6,14,15]

To examine the relationships between the observed site-specific variations in Γ as a function of increasing counterion concentration and the preferential counterion coordination sites for the hairpin, a series of molecular dynamics (MD) simulations of the hairpin in the presence of Na^+ and K^+ were performed. While the MD simulation technique is capable of providing reasonable qualitative predictions of the binding of monovalent cations to nucleic acids, divalent cations are entirely outside the accuracy limits of contemporary simulations.[16] Quantitative analysis of counterion residence times at coordination sites of individual NA bases over the course of the 50 ns MD trajectories was employed to identify preferential coordination sites for Na^+ and K^+ ions. The analysis showed that most of the K^+ ions that broke into the first hydration shell of the NA bases had a mean residence time that was generally shorter than 150 ps (Table S5). However, there were two exceptions: the N3/N7 site of Ade5 and the coordination site formed between the GpC·GpC steps (Figure 2 and Figure S7). At the N3 and N7 sites of Ade5, the mean residence times were approximately 240 and 336 ps, respectively. While the experimental data did not reveal any concentration-dependent perturbations of Ade5 $\Gamma_{C2,C2-H2}$, the signal corresponding to Ade5 H8−C8 was broadened beyond detection in all of the K^+ HSQC spectra (Figure S3). The absence of the Ade5 H8−C8 signal in the 2D HSQC spectrum suggests that Ade5 is involved in slow (microsecond) chemical exchange. Whether this chemical exchange is modulated by the residence time of the coordinated K^+ ions remains obscured from both MD simulations and NMR experiments because of insufficient sampling time and absence of the corresponding NMR signal, respectively. At the site formed between the GpC·GpC steps, K^+ ions were coordinated primarily to the O6 sites of Gua1 and Gua6 and further stabilized by the amino group nitrogens of residues Cyt2 and Cyt7, which together formed a K^+ coordination pocket (Figure S7). A residence time for the coordinated K^+ in this pocket was approximately 250 ps on average (Table S5). Notably, the preferential coordination site at the GpC step agrees with the site indicated by measurements of the K^+ concentration-dependent variations of Γ (Figure 1). The experimentally acquired Γ values showed that Cyt2 and Cyt7 $\Gamma_{C5,C5-H5}$ were most sensitive to K^+ coordination at this site (Figure 1).

An MD simulation of the system in the presence of 300 mM Na^+ indicated that N3 of Ade5 is a primary coordination site and has a Na^+ ion residence time of 310 ps (Table S5). As in the situation in which K^+ is present, the NMR signal corresponding to Ade5 H8−C8 was missing in the HSQC spectra, impeding the unambiguous analysis of the experimental data for this residue (see above). As for the remaining coordination sites, comparison of the MD simulations of d(GCGAAGC) performed in the presence of Na^+ and K^+ revealed a difference in the coordination of Na^+ and K^+, in accordance with the experimental data. Comparison of the average Na^+ residence times revealed two equally preferred coordination sites, namely, N7 of Gua3 and the GpC·GpC pocket (Figure 2 and Table S5). In contrast to K^+, the Na^+ coordination to the GpC·GpC site was diminished, while the residence times of K^+ and Na^+ at N7 of Gua3 were approximately the same (Table S5). The Gua3 $\Gamma_{C8,C8-H8}$ values were more sensitive to Na^+ coordination than were the Cyt2 and Cyt7 $\Gamma_{C5,C5-H5}$ values reporting on the ion coordination to the GpC·GpC step (Figure 1). However, while the Γ experiment positioned the preferential Na^+ coordination site between residues Gua3 and Ade4, the MD data indicated that Na^+ binding to Ade4 was minute (Table S5). To resolve this outward discrepancy, we performed an MD simulation at a lower Na^+ concentration to assess the changes in molecular structure, the ion residence times, and the residue mobilities at the molecular level. A detailed inspection of the differences in the MD trajectories obtained at low and high Na^+ concentrations revealed a pronounced decrease in the Na^+ residence time at Ade4 and a corresponding increase at Ade5 (Table S5). The change in Na^+ concentration also had a marked influence on the fluctuations in the glycosidic torsion angle (χ) of Gua3 and on the stacking arrangement of the Gua3 and Ade4 bases. To provide an independent assessment of the role of mobility changes in the observed Na^+-induced Γ variations, we measured the R_1 and $R_{1\rho}$ relaxation rates (Table S4). As $R_{1\rho}$ carries essentially the same information as Γ and can be additionally influenced by chemical exchange, we relied mostly on R_1 values in the following analysis. Although the Γ and R_1 values are sensitive to S^2 in a similar way, they respond differently to changes in the CSA and τ_c. The only significant observed variation between the R_1 values at low and high Na^+ concentrations was that for C8 of Gua3, for which the R_1 value decreased by ~15%. This observation cannot be fully explained by the slight increase in τ_c accompanying the increase in salt concentration. As the quantum-chemical data indicated only a minute change in the C8 $\sigma_{C,CH}$ upon ion coordination (Table S6), the MD and R_1 data suggest that the observed variation in Γ for Gua3 was primarily due to greater mobility. In contrast, the motion of Ade4 around χ as revealed by MD simulations was virtually unaffected by an increase in Na^+ concentration. As there was no indication of altered mobility for Ade4 from the MD simulation results, the fact that the change in Na^+ concentration produced the site-specific change in Γ but not in R_1 (Figure S6) suggests that the observed change in Γ for Ade4 resulted from changes in $\sigma_{C,CH}$. The alterations in inter-base stacking of Gua3 and Ade4 appear to be the likely source of such changes. Our MD simulations show that the changes in the stacking of Gua3 and Ade4 are correlated with Na^+-induced perturbations in the mobility of Gua3 (Figure S8). Simultaneously, the MD results indicate that neither stacking nor Gua3 mobility perturbations influenced the mobility of

Ade4 (Figure S8). It is known that even small changes in stacking arrangements can be connected with significant differences in the chemical shielding of the base carbons.[17] The combined effect of a slight increase in $\sigma_{C,CH}$ and the expected change in the overall correlation time is entirely consistent with the observed changes in Γ and R_1.

Altogether, the NMR cross-correlated relaxation rates between the aromatic carbon CSA and the proton−carbon vector measured as a function of increasing ion concentration probe both the site-specific response of NA to counterions and the NA rotational tumbling. The technique is extremely sensitive and, as demonstrated here, can be used to detect very weak and transient interactions on a time scale much shorter than τ_c. Such interactions are virtually invisible to conventional NMR techniques such as chemical shift mapping (Figure S4) and NOESY-based techniques,[8] which are not likely to detect ions with occupancy lower than 10%.[15] Notably, both Na^+ and K^+ had occupancies less than 3% in the present study, as indicated by our MD simulations. The use of substitutionary ions such as NH_4^+ would completely miss the differences in binding specificities between physiologically relevant ions such as Na^+ and K^+ found in this study.

Our data also draw attention to the fact that hydrodynamic properties are notably modulated by the nature and concentration of the counterion in the NMR buffer. Although similar observations were made by Fujimioto et al.[18] almost 16 years ago, commonly used hydrodynamics models do not account for the dependence of the hydrodynamic properties of NAs on the type and concentration of the counterions.[19] Our data indicate that τ_c predictions disregarding ion-specific solvation effects might yield correlation times underestimated by up to 20% in comparison with experimental data, depending on the buffer composition employed for the measurements (Figure S2).

■ ASSOCIATED CONTENT

Supporting Information. Materials and methods; theory; experimental Γ, R_1, and $R_{1\rho}$ relaxation rates; 2D $^1H-^{13}C$ HSQC and 1D ^{31}P NMR spectra; H2″(n)−H6/8(n + 1) NOEs; and residence times for Na^+ and K^+ ions from MD simulations of d(GCGAAGC). This material is available free of charge via the Internet at http://pubs.acs.org.

■ AUTHOR INFORMATION

Corresponding Author
fiala@ncbr.chemi.muni.cz; l.trantirek@uu.nl

■ ACKNOWLEDGMENT

This work was supported by grants from the Ministry of Education of the Czech Republic (LC06030 and MSM002-1622413) and the Academy of Sciences of the Czech Republic (AV0Z50040507, AV0Z50040702, and P208/11/1822).

■ REFERENCES

(1) (a) Stellwagen, E.; Muse, J. M.; Stellwagen, N. C. *Biochemistry* **2011**, *50*, 3084. (b) McFail-Isom, L.; Sines, C. C.; Williams, L. D. *Curr. Opin. Struct. Biol.* **1999**, *9*, 298.
(2) Hud, N. V.; Polak, M. *Curr. Opin. Struct. Biol.* **2001**, *11*, 293.
(3) Tan, S.; Davey, C. A. *Curr. Opin. Struct. Biol.* **2011**, *21*, 128.
(4) Halle, B.; Denisov, V. P. *Biopolymers* **1998**, *48*, 210.
(5) Hoogstraten, C. G.; Grant, C. V.; Horton, T. E.; DeRose, V. J.; Britt, R. D. *J. Am. Chem. Soc.* **2002**, *124*, 834.
(6) Egli, M. *Chem. Biol.* **2002**, *9*, 277.
(7) Hud, N. V.; Feigon, J. *Biochemistry* **2002**, *41*, 9900.
(8) Hud, N. V.; Sklenar, V.; Feigon, J. *J. Mol. Biol.* **1999**, *286*, 651.
(9) Kypr, J.; Chládková, J.; Zimulová, M.; Vorlícková, M. *Nucleic Acids Res.* **1999**, *27*, 3466.
(10) Rinnenthal, J.; Richter, C.; Nozinovic, S.; Furtig, B.; Lopez, J. J.; Glaubitz, C.; Schwalbe, H. *J. Biomol. NMR* **2009**, *45*, 143.
(11) Hirao, I.; Kawai, G.; Yoshizawa, S.; Nishimura, Y.; Ishido, Y.; Watanabe, K.; Miura, K. *Nucleic Acids Res.* **1994**, *22*, 576.
(12) Padrta, P.; Štefl, R.; Králík, L.; Žídek, L.; Sklenář, V. *J Biomol. NMR* **2002**, *24*, 1.
(13) Fushman, D.; Tjandra, N.; Cowburn, D. *J. Am. Chem. Soc.* **1998**, *120*, 10947.
(14) Auffinger, P.; Westhof, E. *J. Mol. Biol.* **2000**, *300*, 1113.
(15) Denisov, V. P.; Halle, B. *Proc. Natl. Acad. Sci. U.S.A.* **2000**, *97*, 629.
(16) Ditzler, M. A.; Otyepka, M.; Šponer, J.; Walter, N. G. *Acc. Chem. Res.* **2010**, *43*, 40.
(17) Czernek, J. *J. Phys. Chem. A* **2003**, *107*, 3952.
(18) Fujimoto, B. S.; Miller, J. M.; Ribeiro, N. S.; Schurr, J. M. *Biophys. J.* **1994**, *67*, 304.
(19) Fernandes, M. X.; Ortega, A.; Lopez Martinez, M. C.; Garcia de la Torre, J. *Nucleic Acids Res.* **2002**, *30*, 1782.